Vol 456|13 November 2008|doi:10.1038/nature07473

ARTICLES

Deconstructing voltage sensor function and pharmacology in sodium channels

Frank Bosmans[1,2], Marie-France Martin-Eauclaire[3] & Kenton J. Swartz[1]

Voltage-activated sodium (Na_v) channels are crucial for the generation and propagation of nerve impulses, and as such are widely targeted by toxins and drugs. The four voltage sensors in Na_v channels have distinct amino acid sequences, raising fundamental questions about their relative contributions to the function and pharmacology of the channel. Here we use four-fold symmetric voltage-activated potassium (K_v) channels as reporters to examine the contributions of individual S3b–S4 paddle motifs within Na_v channel voltage sensors to the kinetics of voltage sensor activation and to forming toxin receptors. Our results uncover binding sites for toxins from tarantula and scorpion venom on each of the four paddle motifs in Na_v channels, and reveal how paddle-specific interactions can be used to reshape Na_v channel activity. One paddle motif is unique in that it slows voltage sensor activation, and toxins selectively targeting this motif impede Na_v channel inactivation. This reporter approach and the principles that emerge will be useful in developing new drugs for treating pain and Na_v channelopathies.

Na_v channels in nerve and muscle cells open and close, or 'gate', in response to changes in membrane voltage[1]. Mutations in Na_v channels can cause a variety of inherited disorders, such as epilepsy and myotonia[2,3]. Furthermore, Na_v channels are strategically positioned within nociceptive signalling pathways, with mutations leading to severe pain disorders[4,5]. Although the development of drugs interacting with Na_v channels is of widespread medical importance[6], progress has been slow because the architecture and gating mechanisms of these ion channels are complex. Their channel-forming α-subunits contain four homologous domains (I–IV), or pseudosubunits, each containing six transmembrane segments (S1–S6) (Fig. 1a). The S5–S6 segments collectively form a central pore for Na^+, with the S1–S4 segments from each domain forming the surrounding voltage sensors[1]. Each of the four voltage sensors activate in response to changes in voltage; however, those in domains I–III are most important for channel opening, whereas the one in domain IV is crucial for fast inactivation[7–10]. Thus, drugs and toxins can interact with multiple regions of Na_v channels to influence their activity, with the four voltage sensors representing rich, yet complex targets. The similarity of the four voltage sensors raises the possibility of multiple binding sites, with occupancy of each having distinct effects on gating. Indeed, seven different receptor sites have been proposed for drugs and toxins that interact with Na_v channels[1,11], but only a few have been molecularly defined. Here we develop an approach for studying the unique contributions of the four voltage sensors in Na_v channels to gating and pharmacology. We identify S3b–S4 paddle motifs that can be transplanted from Na_v channels into K_v channels without disrupting function, while transferring sensitivity to classical Na_v channel toxins. Our results uncover rich interactions between toxins and multiple Na_v channel paddle motifs, and reveal how domain-specific interactions can be used to reshape Na_v channel activity.

Transferring paddle motifs between Na_v and K_v channels

Studies on voltage sensors in K_v channels have identified an S3b–S4 helix–turn–helix motif, the voltage-sensor paddle, which moves at the protein–lipid interface to drive activation of the voltage sensors and opening of the pore[12–16]. The paddle motif is an important pharmacological target in K_v channels, as tarantula toxins that partition into membranes interact with this region to inhibit channel opening[12,17–24]. Our initial goal was to determine whether paddle motifs can be defined in Na_v channels and whether they fulfil similar functions. As paddle motifs are portable modules that are interchangeable between K_v channels and voltage-sensing proteins[12], we wondered whether distinct paddle motifs in each of the four voltage sensors of Na_v channels could be transplanted into a homotetrameric K_v channel, so as to study them in isolation (Fig. 1a). We initially transplanted the paddle motifs from $rNa_v1.2a$ and $rNa_v1.4$ channels into the $K_v2.1$ channel (see Methods for nomenclature definition). Although the sequences of these Na_v and K_v channel paddle motifs vary substantially, constructs containing specific S3b–S4 regions of Na_v channels result in fully functional channels that display robust voltage-activated potassium currents (Fig. 1b, c, Supplementary Figs 1, 2a, Supplementary Table 1). Functional chimaeras were also obtained by transplanting the paddle motif from $rNa_v1.4$ into $K_v1.3$ and Shaker K_v channels (Supplementary Figs 1, 2b, c, Supplementary Table 2), demonstrating that paddle motifs of Na_v and K_v channels are generally interchangeable.

Transferring toxin sensitivity between Na_v and K_v channels

We next asked whether transplanting isolated paddle motifs from Na_v channels into K_v channels faithfully transfers sensitivity to toxins, in which case the K_v channel could be used as a reporter for investigating interactions between toxins and individual Na_v channel paddle motifs. Tarantula toxins related to those targeting paddle motifs in K_v channels[12,17–22,24] (Supplementary Fig. 1d) inhibit Na_v channels by modifying gating[25–27], but their presumed receptors within the four voltage sensors of Na_v channels have yet to be defined. We focused on three tarantula toxins, PaurTx3, ProTx-I and ProTx-II[25–27], and tested whether they interact with the $K_v2.1$ channel containing each of the four paddle motifs from $rNa_v1.2a$. Remarkably,

[1]Molecular Physiology and Biophysics Section, Porter Neuroscience Research Center, National Institute of Neurological Disorders and Stroke, National Institutes of Health, Bethesda, Maryland 20892, USA. [2]Laboratory of Toxicology, University of Leuven, 3000 Leuven, Belgium. [3]CNRS UMR 6231, CRN2M, Institut Jean Roche, Université de la Méditerranée, Marseille Cedex 20, France.

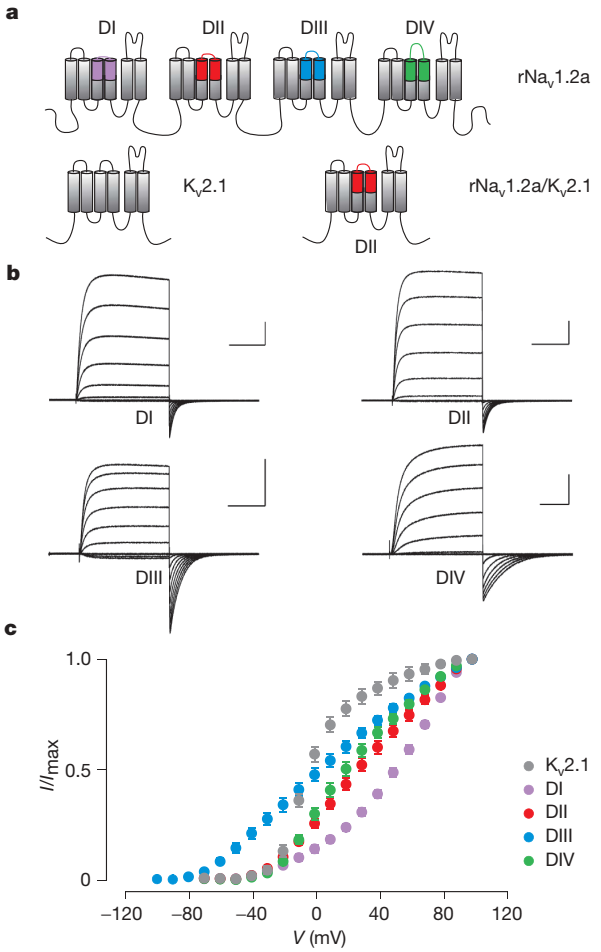

Figure 1 | Transfer of the voltage sensor paddle motifs from rNa$_v$1.2a to K$_v$2.1. **a**, Cartoon depicting the paddle motif transfer from the Na$_v$ channel S1–S4 voltage sensor of domain II into K$_v$2.1. Purple, domain I paddle (DI); red, domain II paddle (DII); blue, domain III paddle (DIII); green, domain IV paddle (DIV). This colour code is used in all figures. **b**, **c**, Families of potassium currents (**b**) and tail current voltage-activation relationships (**c**) for each chimaera ($n = 18$; error bars, s.e.m.). Holding voltage was −90 mV and the tail voltage was −50 mV (−80 mV for DIII). Scale bars (**b**) are 2 μA (vertical) and 100 ms (horizontal).

sensitivity to these toxins can be transferred to K$_v$2.1 along with specific Na$_v$ channel paddle motifs (Fig. 2a). PaurTx3 has the simplest profile of the three, as this toxin only inhibits the K$_v$ channel containing the paddle motif from domain II (Fig. 2a, Supplementary Fig. 3a, Supplementary Table 3). In contrast, ProTx-I and ProTx-II interact with multiple paddle motifs from rNa$_v$1.2a. ProTx-I binds to K$_v$2.1 containing the paddle motifs from domain II or IV, whereas ProTx-II interacts with those from domains I, II or IV. (ProTx-I also inhibits K$_v$2.1 (ref. 26), but the lack of toxin sensitivity for the domain I and III chimaeras support interaction of the toxin with paddle motifs.) Although it is not straightforward to directly correlate the apparent affinities of K$_v$ channel paddle chimaeras and Na$_v$ channels because the paddles are identical in K$_v$ channels and different in Na$_v$ channels, the concentration-dependence for toxin inhibition of the two channel types are remarkably similar (Supplementary Fig. 4a, b, Supplementary Table 3). These results show that tarantula toxins often interact with multiple paddle motifs in Na$_v$ channels, a scenario that would be difficult to detect using conventional approaches[27,28].

Studies on scorpion venom have established the presence of two classes of toxins, the α- and β-scorpion toxins, that interact with the voltage sensors in domains IV and II of Na$_v$ channels, respectively[1,29–33]. In the conventional view, these toxins interact with solvent-exposed extracellular loops between S3 and S4 to stabilize the voltage sensors in specific states[8,31,34]. Whether these toxins interact with the larger S3b–S4 paddle motif, or can target voltage sensors in domains other than II and IV, is unknown. To explore these possibilities we tested whether we could make K$_v$2.1 sensitive to the classical α- and β-scorpion toxins. As in the case of tarantula toxins, transfer of Na$_v$ channel paddle motifs into K$_v$2.1 renders the channel sensitive to the α-scorpion toxin AaHII; however, in this instance only the paddle motif from domain IV can transfer toxin sensitivity (Fig. 2a, Supplementary Fig. 3a). Although the apparent affinity of AaHII for the domain IV chimaera is considerably less than for rNa$_v$1.2a (Supplementary Fig. 4d, Supplementary Table 3), mutations within S4 can increase the apparent affinity by over 10-fold (Figs 3d, 4c, Supplementary Fig. 4d). These results suggest that α-scorpion toxins interact with the paddle motif from domain IV, but the modest affinity of the paddle chimaera leaves open the possibility that other regions of Na$_v$ channels contribute to the toxin receptor[35].

We also examined whether sensitivity to the β-scorpion toxin TsVII could be transferred with Na$_v$ channel paddle motifs. In contrast to AaHII, transfer of the paddle motifs from domains II, III or IV from rNa$_v$1.2a renders the K$_v$ channel sensitive to TsVII (Fig. 2a, Supplementary Fig. 3a), revealing that β-scorpion toxins can interact

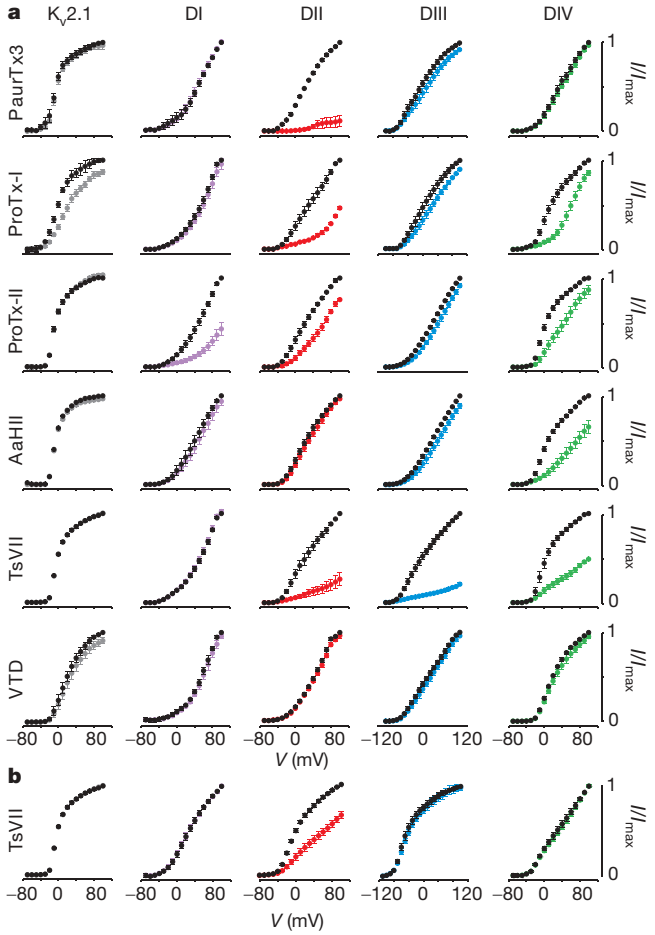

Figure 2 | Sensitivity of rNa$_v$1.2a paddle chimaeras to extracellular toxins. **a**, Effects of toxins on K$_v$2.1 and chimaeras where paddle motifs were transferred from rNa$_v$1.2a into K$_v$2.1. Normalized tail current voltage-activation relationships are shown, where tail current amplitude (I/I_{max}) is plotted against test voltage before (black) and in the presence of toxins (other colours). Data are grouped per toxin (horizontally; toxin named at left) and per chimaera or wild-type K$_v$2.1 (vertically; see labels at top). Concentrations used are 100 nM (PaurTx3, ProTx-I and ProTx-II); 1 μM (AaHII); 500 nM (TsVII) and 100 μM (veratridine; VTD). The plant alkaloid VTD is used as a negative control. **b,** Effects of TsVII (50 nM) on rNa$_v$1.4 paddle chimaeras. $n = 3–5$; error bars, s.e.m. The holding voltage was −90 mV, the test pulse duration was 300 ms and the tail voltage was −50 mV (−80 mV for DIII).

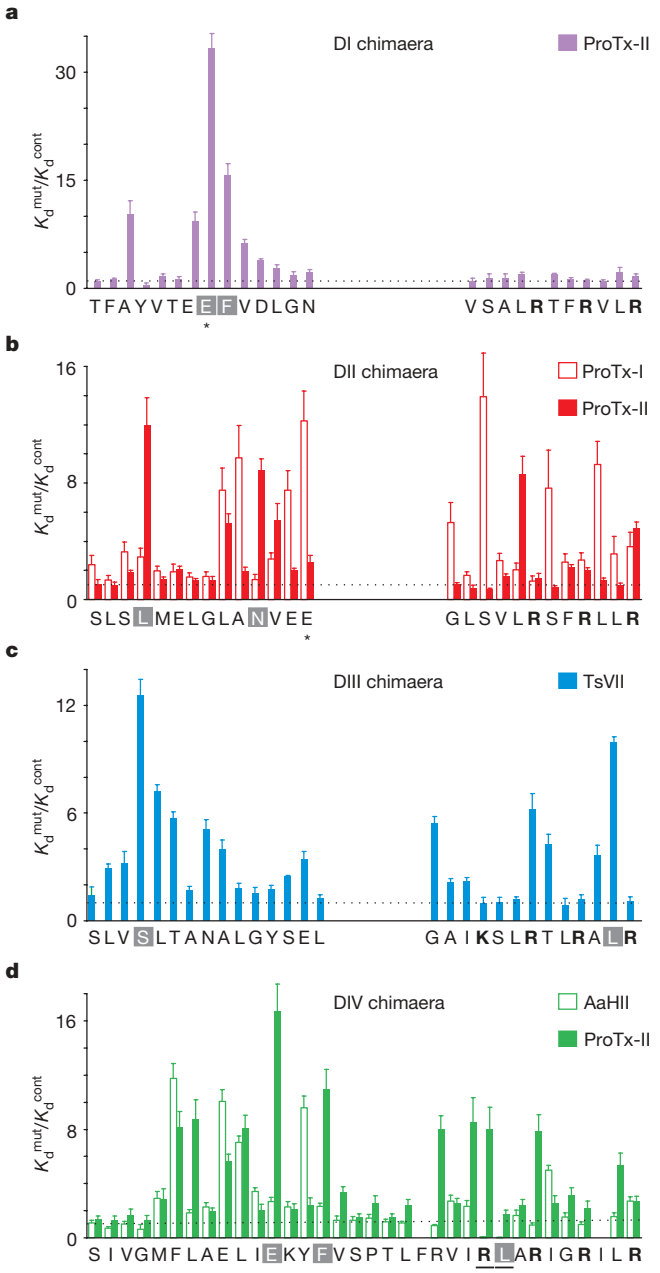

Figure 3 | Scanning mutagenesis of Na_v channel paddle motifs. **a**–**d**, Ala-scan (see below) of the separate $rNa_v1.2a$ paddle motifs in the DI–DIV chimaeras; changes in apparent toxin affinity (K_d^{mut}/K_d^{cont}) are plotted for individual mutants. See Methods, Supplementary Figs 4, 5c, and Supplementary Table 3 for information on K_d measurements. Most of the residues within the $rNa_v1.2a$ paddle in the four chimaera constructs were individually mutated to Ala (except for native Ala residues, which were mutated to Val). The dashed line marks a value of 1. Each mutant was initially examined using a concentration near the K_d value determined for the control chimaera (Supplementary Fig. 4). Mutants with a K_d^{mut}/K_d^{cont} value greater than five were further examined using a wider range of concentrations. Glu residues marked with asterisks were also mutated to a Lys. Bar diagrams are approximately aligned according to the sequence alignment of the different paddles (Supplementary Fig. 1). Mutants without a corresponding bar did not result in functional channels. Residues with a grey background were used in subsequent tests (Fig. 4). Mutation of two underlined residues in **d** results in an increase in AaHII affinity (K_d = 235 ± 24 nM for R1629A, 205 ± 23 nM for L1630A and 1,902 ± 102 nM for the DIV chimera). Basic residues in S4 were used to align the sequences and are indicated in bold. n = 3–5 for each toxin concentration; error bars, s.e.m.

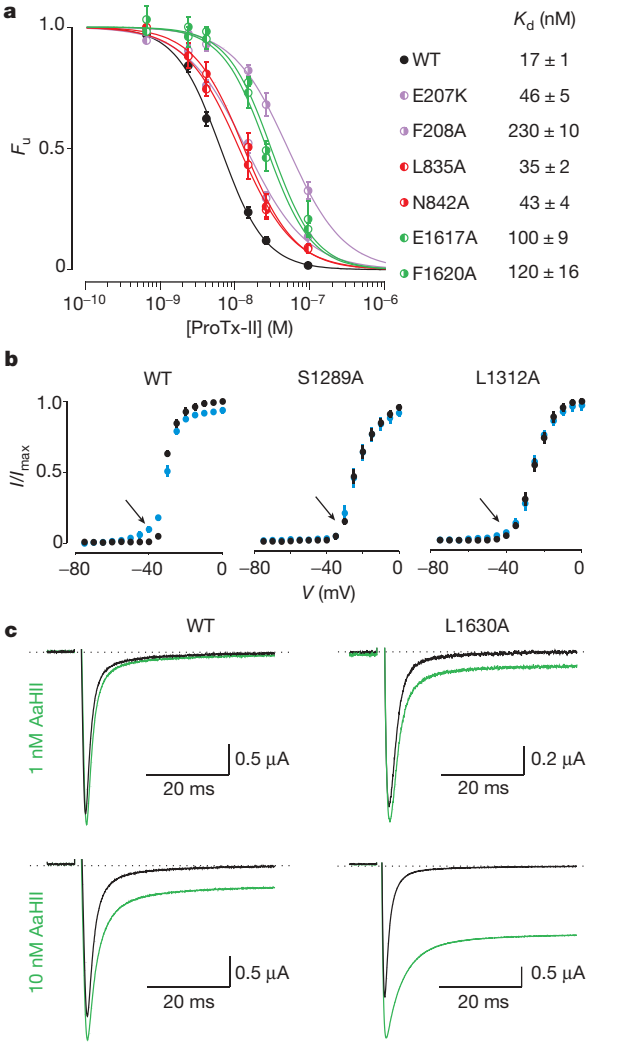

Figure 4 | Reconstitution of paddle mutants into $rNa_v1.2a$ and their effects on toxin–channel interactions. **a**, Concentration dependence for ProTx-II inhibition of $rNa_v1.2a$ (WT) and selected mutants plotted as fraction unbound (F_u) measured at negative voltages. Solid lines are fits of the Hill equation to the data with apparent K_d values shown. See Supplementary Fig. 5b and Supplementary Table 3 for further information. **b**, Normalized conductance–voltage relationships for $rNa_v1.2a$ and two DIII mutants before and after addition of 50 nM TsVII. Arrow indicates toxin effect or lack thereof. Holding voltage was −90 mV. **c**, $rNa_v1.2a$ mutation L1630A increases affinity for AaHII. Sodium currents were elicited by a depolarization to −15 mV from a holding voltage of −90 mV. Green trace is after AaHII addition. Error bars (**a**, **b**), s.e.m.

with multiple Na_v channel paddle motifs. This result is surprising, because studies on $rNa_v1.4$ suggest that TsVII only binds to the voltage sensor in domain II[36,37]. To explore whether scorpion toxin interactions vary between Na_v channel subtypes, we tested the sensitivity of the $rNa_v1.4$ paddle chimaeras to TsVII. By contrast with what is observed with the $rNa_v1.2a$ paddles, TsVII can interact selectively with the domain II paddle from $rNa_v1.4$ (Fig. 2b, Supplementary Fig. 3b). Although the apparent affinities of TsVII for the $rNa_v1.2a$ paddle chimaeras are significantly lower than the $rNa_v1.2a$ channel, the $rNa_v1.4$ domain II paddle chimaera is comparable (Supplementary Fig. 4c, Supplementary Table 3). An interesting feature of TsVII is that the β-scorpion toxin stabilizes a closed state in the paddle chimaeras (Fig. 2), whereas the toxin stabilizes the open state of $rNa_v1.2a$ (Fig. 4b) and $rNa_v1.4$ (ref. 37) channels. β-scorpion toxins can also stabilize a closed state in certain Na_v channels[32], indicating that open state stabilization is not always observed. One explanation is that toxin binding to the paddle

intrinsically stabilizes a closed state, but in certain Na_v channels the toxin can stabilize an open state when it also interacts with other regions[32,33]. Taken together, these data suggest that both tarantula and scorpion toxins interact with paddle motifs, that multiple paddle motifs can be targeted by individual toxins, and that these interactions can differ between Na_v channel subtypes.

Critical residues in the toxin–paddle interaction

To further explore the extent to which toxins interact with S3b–S4 paddle motifs, and to identify mutants for testing whether these toxin–paddle interactions actually occur in Na_v channels, we mutated each residue in the transferred paddle regions and measured changes in toxin affinity (Fig. 3, Supplementary Fig. 4, Supplementary Tables 4–7). One striking feature of the data is that mutations distributed throughout the S3b–S4 paddle motifs cause dramatic perturbations in the apparent affinity for both tarantula and scorpion toxins, suggesting that these toxins target the larger paddle motif. Many of the most influential mutations are of hydrophobic residues, but mutations of polar residues such as Glu residues in S3b and Arg residues in S4 also have pronounced effects. The present mutagenesis of the domain IV paddle motif correctly identifies several mutants previously shown to weaken α-scorpion toxin affinity in Na_v channels[31], but reveals a larger number of influential mutations, many of which have more pronounced effects on toxin affinity. This highlights an advantage of the reporter approach, which allows individual toxin–paddle interactions to be studied in isolation; toxins can interact with up to four different paddle motifs in Na_v channels and the effects of mutations in any one of those can be quite subtle because the others remain unaltered.

Another striking feature of these paddle scans is that mutations perturbing toxin–paddle interactions are unique for each toxin–paddle pair. For example, both ProTx-I and ProTx-II interact with the paddle motif from domain II, but the mutants that weaken toxin affinity only partially overlap. In addition, the mutagenesis results for ProTx-II interacting with paddle motifs from domains I, II and IV identify many influential mutations that differ between the three paddles. This comparison suggests that toxin–paddle interactions do not obey a general lock-and-key mechanism, but that the interfaces vary considerably.

Validating toxin-paddle interactions in $rNa_v1.2a$

To validate that the toxin–paddle interactions identified here actually occur in Na_v channels, we reconstituted the most influential paddle mutants into $rNa_v1.2a$ and measured changes in toxin affinity. For tarantula toxins, we examined mutations influencing ProTx-II affinity, as this toxin interacts with three of the four Na_v channel paddle motifs. Mutations within the paddle motifs of domains I, II and IV weaken the interaction of ProTx-II with $rNa_v1.2$ (Fig. 4a), suggesting that the toxin interacts with all three paddle motifs in the Na_v channel. The mutations tend to have smaller effects in the Na_v channel when compared with the paddle chimaeras (compare Fig. 4a with Fig. 3a, b, d), which makes sense because the mutations in the Na_v channel alter only one of three targeted paddle motifs, whereas in the K_v channel chimaera they alter all four. For the β-scorpion toxin TsVII, we examined mutations within the paddle motif of domain III and found that they diminish the hyperpolarizing shift produced by moderate toxin concentrations (Fig. 4b), confirming that the toxin interacts with domain III (in addition to its canonical interaction with domain II). Finally, in the case of the α-scorpion toxin AaHII, we reconstituted a gain-of-function mutation into $rNa_v1.2a$ and observed that the mutation also increases the apparent affinity of the toxin in the Na_v channel (Fig. 4c). These results demonstrate that the toxin–paddle interactions uncovered using the reporter approach actually occur in Na_v channels.

Unique character of the domain IV paddle motif

The differential coupling of the four voltage sensors in Na_v channels to opening and inactivation[8,10,38–40] is accompanied by differences in the kinetics of voltage sensor activation, with the voltage sensor of domain IV moving slower than the other three[10]. Given that the paddle motif resides in a relatively unconstrained environment in contact with the surrounding lipid membrane, and that it is the region of the voltage sensor that flexes in response to changes in voltage[12–16,41], we wondered whether the paddle motif itself might be responsible for these kinetic differences. To explore this possibility, we measured the kinetics of activation (opening) and deactivation (closing) of the four $rNa_v1.2a$ paddle chimaeras in $K_v2.1$ in response to membrane depolarization and repolarization, respectively (Fig. 5). At most voltages, the time

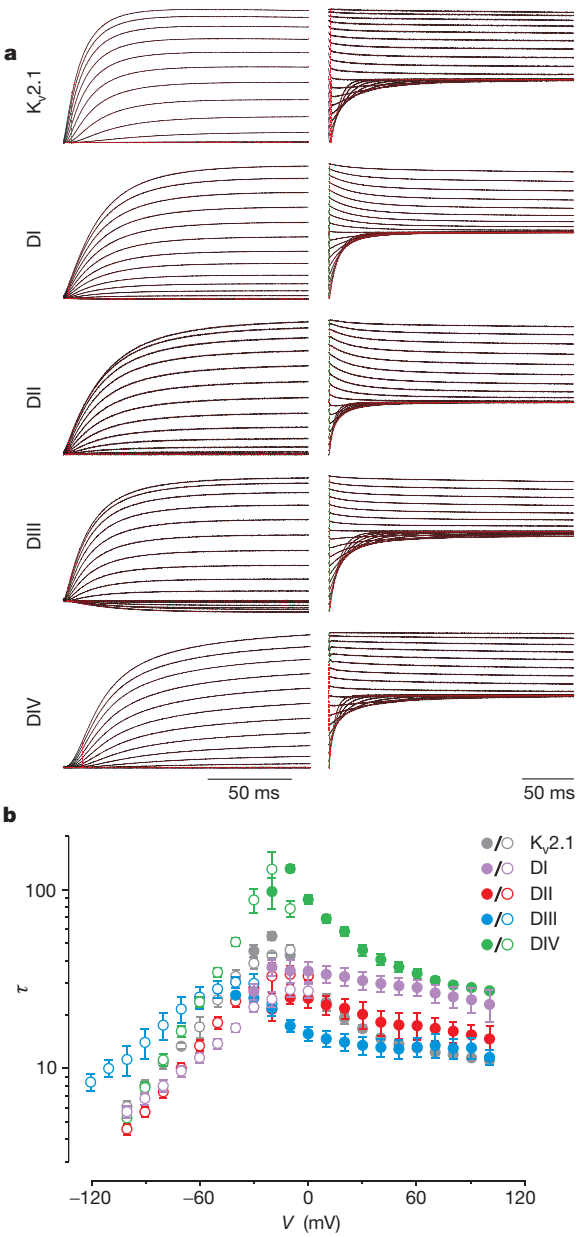

Figure 5 | Kinetics of opening and closing for $rNa_v1.2a/K_v2.1$ chimaeras. **a**, Representative macroscopic currents (black) showing channel activation (left) and channel deactivation (right) using the following voltage protocols: activation, 10 mV incrementing steps to voltages between −40 mV and +100 mV from a holding potential of −90 mV; deactivation, 10 mV incrementing steps to voltages between 0 mV and −100 mV (−120 mV for DIII) from a test voltage of between +80 mV and +100 mV (holding potential is −90 mV). Superimposed red curves are single exponential fits to the current records after initial lags in current activation. **b,** Mean time constants (τ) from single exponential fits to channel activation (filled circles) and deactivation (open circles) plotted as a function of the voltage at which the current was recorded. $n = 4–8$; error bars, s.e.m.

constants obtained by fitting single exponential functions to current relaxations are notably slower for the domain IV paddle chimaera compared with the other chimaeras and to K_v2.1. This difference is not unique to chimaeras between the rNa$_v$1.2a and K_v2.1 channel, but is even more pronounced when transplanting paddle motifs from rNa$_v$1.4 into K_v2.1, K_v1.3 or Shaker K_v channels (Supplementary Fig. 2). These results demonstrate that the paddle motif in domain IV of Na$_v$ channels determines the slower movement of this voltage sensor in response to changes in membrane voltage.

Shaping Na$_v$ channel activity with domain-selective interactions

A particularly intriguing outcome of looking at toxin–paddle interactions in isolation is that patterns emerge between the domains targeted and the effects of the toxin on Na$_v$ channel activity. Inspection of the profiles for toxin–paddle interactions (Fig. 2) reveals that by targeting paddle motifs in domains I, II or III, the overall effect of a toxin is to influence opening of Na$_v$ channels, irrespective of whether domain IV is also targeted. The tarantula toxins PaurTx3, ProTx-I and ProTx-II, as well as the β-scorpion toxin TsVII, are examples of this relationship. In contrast, the requirements for influencing inactivation are more stringent; to do so, a toxin needs to selectively target the paddle motif in domain IV, as is the case with the α-scorpion toxin AaHII. To test whether this pattern is generally applicable across different toxin families, we searched for a tarantula toxin that selectively interacts with the paddle motif in domain IV and asked whether it influences inactivation. Using our reporter constructs, we screened various tarantula toxins, including VSTx1 (ref. 42), GxTx-1E (ref. 43), HaTx (ref. 18) and SGTx1 (ref. 44), all of which interact with paddle motifs in K_v channels[12,17–21,24,44] and are related in sequence to the Na$_v$ channel toxins already studied (Supplementary Fig. 1d). VSTx1 (10 μM) and GxTx-1E (500 nM) are inactive against the Na$_v$ paddle chimaeras (not shown), whereas both HaTx and SGTx1 exhibit robust effects (Fig. 6a). HaTx interacts with paddle motifs from domains I, II and IV, similarly to ProTx-II, whereas SGTx1 interacts selectively with the domain IV paddle chimaera, the profile we sought to find. When tested against rNa$_v$1.2a, HaTx exhibits robust inhibitory effects, similar to ProTx-II, without significantly altering inactivation (Fig. 6b). In contrast, SGTx1 does not inhibit rNa$_v$1.2a or alter channel opening, but dramatically reduces the extent of inactivation (Fig. 6c), behaving as an α-scorpion toxin. These results suggest that for a toxin to influence inactivation, it must selectively interact with the paddle motif in domain IV; any additional interactions with the other paddles will alter channel opening.

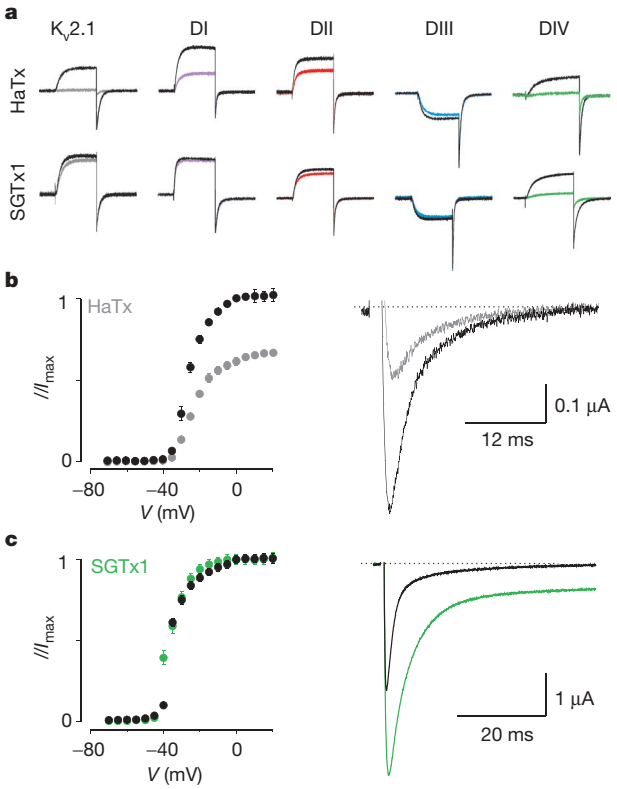

Figure 6 | Identifying a tarantula toxin selective for the paddle motif in domain IV. a, Potassium currents elicited by depolarizations near the foot of the voltage-activation curve for K_v2.1 and chimaeras in the absence and presence of 50 nM HaTx or 100 nM SGTx1. The holding voltage was −90 mV, the test pulse duration was 300 ms and the tail voltage was −50 mV (−80 mV for DIII). **b**, Left, conductance–voltage relationships for rNa$_v$1.2a before and after addition of 50 nM HaTx, normalized to the maximal conductance in control. Right, sodium current elicited by a depolarization to −30 mV before and after addition of 50 nM HaTx. **c**, Left, conductance–voltage relationship of rNa$_v$1.2a before and after addition of 100 nM SGTx1, individually normalized to the maximal conductance in either control or the presence of toxin. Right, sodium current elicited by a depolarization to −15 mV before and after addition of 100 nM SGTx1. n = 3–5 for each toxin concentration; error bars (**b**, **c**), s.e.m.

Discussion

Our results on isolating Na$_v$ channel paddle motifs using K_v channels as reporters have three fundamental implications for the function and pharmacology of Na$_v$ channels. First, they reveal that paddle motifs can determine the kinetics of voltage sensor activation. For Na$_v$ channels to function properly, inactivation must proceed more slowly than opening, a property that has been attributed to slower activation of the voltage sensor in domain IV[1,8,10,38,45]. Our results show that the paddle motif in domain IV is unique because it systematically slows activation of any voltage sensor into which it is incorporated (Fig. 5, Supplementary Fig. 2). The paddle motif resides in a relatively flexible environment and moves in contact with the surrounding lipid membrane[12–16,41], raising the intriguing possibility that interactions of the domain IV paddle motif with lipids are unique and are responsible for slowing voltage sensor activation. Other aspects of Na$_v$ channel function are unlikely to be determined by the paddle motif (for example, cooperative voltage sensor activation[10,37,46]), but the approaches described here may help to identify them.

Second, our results reveal rich interactions of tarantula and scorpion toxins with paddle motifs, and establish a number of principles for toxin–paddle interactions in Na$_v$ channels where the four paddle motifs are not equivalent. Although α- and β-scorpion toxins are known to interact with domains IV and II, respectively[31,32], the present results demonstrate that each of the paddle motifs are targeted by toxins (Fig. 2). In fact, multiple paddle motifs are often targeted by a toxin. Even the β-scorpion toxins can interact with other domains in addition to the canonical interaction with domain II. One unexpected finding is that the profiles of toxin–paddle interactions can differ between subtypes of Na$_v$ channels, suggesting that such profiles may be a way of distinguishing Na$_v$ channels. Our mutagenesis results with the four paddle motifs in rNa$_v$1.2a also show that the pattern of mutants altering toxin affinity is specific for each toxin–paddle pair (Fig. 3). The most influential mutants can vary considerably for one toxin interacting with different paddles, or for two related toxins interacting with a single paddle motif.

Last, the profiles of toxin–paddle interactions that emerge from our studies reveal an important relationship between the effect of a toxin on Na$_v$ channel activity and domain-specific interactions. Alterations in channel opening can be achieved with molecules that interact with any of the first three paddle motifs in Na$_v$ channels without regard for whether domain IV is also targeted (for example HaTx, ProTx-II, TsVII), whereas influencing inactivation requires that a molecule interact exclusively with the paddle in domain IV (for example SGTX1, AaHII). These domain-specific interactions have important

implications for designing drugs to reshape Na_v channel activity. Channelopathies like idiopathic ventricular fibrillation[47] and long QT syndrome type 3 (ref. 48) are associated with accelerated Na_v channel inactivation, which could be restored by selectively targeting the domain IV paddle motif. In contrast, the hyperpolarization of Na_v channel opening seen in disorders like generalized epilepsy with febrile seizures type 2 (ref. 49) and hyperkalaemic periodic paralysis[50] could be managed with drugs targeting any paddle motif within the first three domains. Our reporter approach for identifying toxins that specifically target the paddle motif in domain IV (Fig. 6) provides a conceptual example for identifying drugs that interact with specific paddle motifs in Na_v channels.

METHODS SUMMARY

Channel constructs were expressed in *Xenopus* oocytes[21] and studied using two-electrode voltage-clamp recording techniques. Na_v channels were co-expressed with the β_1 subunit. For K_v channel experiments, the external recording solution contained 50 mM KCl, 50 mM NaCl, 5 mM HEPES, 1 mM $MgCl_2$ and 0.3 mM $CaCl_2$, pH 7.6 with NaOH. KCl was replaced by RbCl for Shaker experiments. For Na_v channel experiments, the external recording solution contained 96 mM NaCl, 2 mM KCl, 5 mM HEPES, 1 mM $MgCl_2$ and 1.8 mM $CaCl_2$, pH 7.6 with NaOH.

Voltage–activation relationships were obtained by measuring tail currents for K_v channels or steady-state currents and calculating conductance for Na_v channels, and a single Boltzmann function was fitted to the data. Occupancy of closed or resting channels by toxins was examined using negative holding voltages where open probability was low, and the fraction of unbound channels (F_u) was estimated using depolarizations that are too weak to open toxin-bound channels, as described previously[17–21,24,44]. The apparent equilibrium dissociation constant (K_d) for toxin interaction with K_v channel constructs was calculated assuming four independent toxin-binding sites per channel, with single occupancy being sufficient to inhibit opening in response to weak depolarizations (see Methods, Supplementary Figs 4, 5c and Supplementary Table 3 for information on K_d measurements).

Full Methods and any associated references are available in the online version of the paper at www.nature.com/nature.

Received 22 August; accepted 30 September 2008.

1. Catterall, W. A. From ionic currents to molecular mechanisms: The structure and function of voltage-gated sodium channels. *Neuron* **26,** 13–25 (2000).
2. Cannon, S. C. Pathomechanisms in channelopathies of skeletal muscle and brain. *Annu. Rev. Neurosci.* **29,** 387–415 (2006).
3. George, A. L. Jr. Inherited disorders of voltage-gated sodium channels. *J. Clin. Invest.* **115,** 1990–1999 (2005).
4. Cox, J. J. *et al.* An SCN9A channelopathy causes congenital inability to experience pain. *Nature* **444,** 894–898 (2006).
5. Fertleman, C. R. *et al.* SCN9A mutations in paroxysmal extreme pain disorder: Allelic variants underlie distinct channel defects and phenotypes. *Neuron* **52,** 767–774 (2006).
6. Kaczorowski, G. J., McManus, O. B., Priest, B. T. & Garcia, M. L. Ion channels as drug targets: The next GPCRs. *J. Gen. Physiol.* **131,** 399–405 (2008).
7. Horn, R., Ding, S. & Gruber, H. J. Immobilizing the moving parts of voltage-gated ion channels. *J. Gen. Physiol.* **116,** 461–476 (2000).
8. Sheets, M. F., Kyle, J. W., Kallen, R. G. & Hanck, D. A. The Na channel voltage sensor associated with inactivation is localized to the external charged residues of domain IV, S4. *Biophys. J.* **77,** 747–757 (1999).
9. Yang, N. & Horn, R. Evidence for voltage-dependent S4 movement in sodium channels. *Neuron* **15,** 213–218 (1995).
10. Chanda, B. & Bezanilla, F. Tracking voltage-dependent conformational changes in skeletal muscle sodium channel during activation. *J. Gen. Physiol.* **120,** 629–645 (2002).
11. Catterall, W. A. *et al.* Voltage-gated ion channels and gating modifier toxins. *Toxicon* **49,** 124–141 (2007).
12. Alabi, A. A., Bahamonde, M. I., Jung, H. J., Kim, J. I. & Swartz, K. J. Portability of paddle motif function and pharmacology in voltage sensors. *Nature* **450,** 370–375 (2007).
13. Chakrapani, S., Cuello, L. G., Cortes, D. M. & Perozo, E. Structural dynamics of an isolated voltage-sensor domain in a lipid bilayer. *Structure* **16,** 398–409 (2008).
14. Jiang, Y. *et al.* X-ray structure of a voltage-dependent K^+ channel. *Nature* **423,** 33–41 (2003).
15. Jiang, Y., Ruta, V., Chen, J., Lee, A. & MacKinnon, R. The principle of gating charge movement in a voltage-dependent K^+ channel. *Nature* **423,** 42–48 (2003).
16. Ruta, V., Chen, J. & MacKinnon, R. Calibrated measurement of gating-charge arginine displacement in the KvAP voltage-dependent K^+ channel. *Cell* **123,** 463–475 (2005).
17. Swartz, K. J. & MacKinnon, R. Mapping the receptor site for hanatoxin, a gating modifier of voltage-dependent K^+ channels. *Neuron* **18,** 675–682 (1997).
18. Swartz, K. J. & MacKinnon, R. Hanatoxin modifies the gating of a voltage-dependent K^+ channel through multiple binding sites. *Neuron* **18,** 665–673 (1997).
19. Li-Smerin, Y. & Swartz, K. J. Gating modifier toxins reveal a conserved structural motif in voltage-gated Ca^{2+} and K^+ channels. *Proc. Natl Acad. Sci. USA* **95,** 8585–8589 (1998).
20. Li-Smerin, Y. & Swartz, K. J. Localization and molecular determinants of the Hanatoxin receptors on the voltage-sensing domains of a K(+) channel. *J. Gen. Physiol.* **115,** 673–684 (2000).
21. Lee, H. C., Wang, J. M. & Swartz, K. J. Interaction between extracellular Hanatoxin and the resting conformation of the voltage-sensor paddle in Kv channels. *Neuron* **40,** 527–536 (2003).
22. Lee, S. Y. & MacKinnon, R. A membrane-access mechanism of ion channel inhibition by voltage sensor toxins from spider venom. *Nature* **430,** 232–235 (2004).
23. Milescu, M. *et al.* Tarantula toxins interact with voltage sensors within lipid membranes. *J. Gen. Physiol.* **130,** 497–511 (2007).
24. Phillips, L. R. *et al.* Voltage-sensor activation with a tarantula toxin as cargo. *Nature* **436,** 857–860 (2005).
25. Bosmans, F. *et al.* Four novel tarantula toxins as selective modulators of voltage-gated sodium channel subtypes. *Mol. Pharmacol.* **69,** 419–429 (2006).
26. Middleton, R. E. *et al.* Two tarantula peptides inhibit activation of multiple sodium channels. *Biochemistry* **41,** 14734–14747 (2002).
27. Smith, J. J., Cummins, T. R., Alphy, S. & Blumenthal, K. M. Molecular interactions of the gating modifier toxin ProTx-II with NaV 1.5: Implied existence of a novel toxin binding site coupled to activation. *J. Biol. Chem.* **282,** 12687–12697 (2007).
28. Sokolov, S., Kraus, R. L., Scheuer, T. & Catterall, W. A. Inhibition of sodium channel gating by trapping the domain II voltage sensor with protoxin II. *Mol. Pharmacol.* **73,** 1020–1028 (2008).
29. Cahalan, M. D. Modification of sodium channel gating in frog myelinated nerve fibres by *Centruroides sculpturatus* scorpion venom. *J. Physiol. (Lond.)* **244,** 511–534 (1975).
30. Koppenhofer, E. & Schmidt, H. Effect of scorpion venom on ionic currents of the node of Ranvier. II. Incomplete sodium inactivation. *Pflugers Arch.* **303,** 150–161 (1968).
31. Rogers, J. C., Qu, Y., Tanada, T. N., Scheuer, T. & Catterall, W. A. Molecular determinants of high affinity binding of alpha-scorpion toxin and sea anemone toxin in the S3-S4 extracellular loop in domain IV of the Na^+ channel alpha subunit. *J. Biol. Chem.* **271,** 15950–15962 (1996).
32. Cestele, S. *et al.* Voltage sensor-trapping: Enhanced activation of sodium channels by beta-scorpion toxin bound to the S3-S4 loop in domain II. *Neuron* **21,** 919–931 (1998).
33. Cestele, S. *et al.* Structure and function of the voltage sensor of sodium channels probed by a beta-scorpion toxin. *J. Biol. Chem.* **281,** 21332–21344 (2006).
34. Cohen, L. *et al.* Direct evidence that receptor site-4 of sodium channel gating modifiers is not dipped in the phospholipid bilayer of neuronal membranes. *J. Biol. Chem.* **281,** 20673–20679 (2006).
35. Tejedor, F. J. & Catterall, W. A. Site of covalent attachment of alpha-scorpion toxin derivatives in domain I of the sodium channel alpha subunit. *Proc. Natl Acad. Sci. USA* **85,** 8742–8746 (1988).
36. Marcotte, P., Chen, L. Q., Kallen, R. G. & Chahine, M. Effects of *Tityus serrulatus* scorpion toxin gamma on voltage-gated Na^+ channels. *Circ. Res.* **80,** 363–369 (1997).
37. Campos, F. V., Chanda, B., Beirao, P. S. & Bezanilla, F. Beta-scorpion toxin modifies gating transitions in all four voltage sensors of the sodium channel. *J. Gen. Physiol.* **130,** 257–268 (2007).
38. Campos, F. V., Chanda, B., Beirao, P. S. & Bezanilla, F. Alpha-scorpion toxin impairs a conformational change that leads to fast inactivation of muscle sodium channels. *J. Gen. Physiol.* **132,** 251–263 (2008).
39. Cha, A., Ruben, P. C., George, A. L. Jr, Fujimoto, E. & Bezanilla, F. Voltage sensors in domains III and IV, but not I and II, are immobilized by Na^+ channel fast inactivation. *Neuron* **22,** 73–87 (1999).
40. Sheets, M. F., Kyle, J. W. & Hanck, D. A. The role of the putative inactivation lid in sodium channel gating current immobilization. *J. Gen. Physiol.* **115,** 609–620 (2000).
41. Banerjee, A. & MacKinnon, R. Inferred motions of the S3a helix during voltage-dependent K^+ channel gating. *J. Mol. Biol.* **381,** 569–580 (2008).
42. Ruta, V., Jiang, Y., Lee, A., Chen, J. & MacKinnon, R. Functional analysis of an archaebacterial voltage-dependent K^+ channel. *Nature* **422,** 180–185 (2003).
43. Herrington, J. *et al.* Blockers of the delayed-rectifier potassium current in pancreatic beta-cells enhance glucose-dependent insulin secretion. *Diabetes* **55,** 1034–1042 (2006).
44. Lee, C. W. *et al.* Solution structure and functional characterization of SGTx1, a modifier of Kv2.1 channel gating. *Biochemistry* **43,** 890–897 (2004).
45. Armstrong, C. M. Na channel inactivation from open and closed states. *Proc. Natl Acad. Sci. USA* **103,** 17991–17996 (2006).
46. Chanda, B., Asamoah, O. K. & Bezanilla, F. Coupling interactions between voltage sensors of the sodium channel as revealed by site-specific measurements. *J. Gen. Physiol.* **123,** 217–230 (2004).

47. Wan, X., Chen, S., Sadeghpour, A., Wang, Q. & Kirsch, G. E. Accelerated inactivation in a mutant Na(+) channel associated with idiopathic ventricular fibrillation. *Am. J. Physiol. Heart Circ. Physiol.* **280,** H354–H360 (2001).
48. Bennett, P. B., Yazawa, K., Makita, N. & George, A. L. Jr. Molecular mechanism for an inherited cardiac arrhythmia. *Nature* **376,** 683–685 (1995).
49. Spampanato, J., Escayg, A., Meisler, M. H. & Goldin, A. L. Generalized epilepsy with febrile seizures plus type 2 mutation W1204R alters voltage-dependent gating of Na(v)1.1 sodium channels. *Neuroscience* **116,** 37–48 (2003).
50. Bendahhou, S., Cummins, T. R., Tawil, R., Waxman, S. G. & Ptacek, L. J. Activation and inactivation of the voltage-gated sodium channel: Role of segment S5 revealed by a novel hyperkalaemic periodic paralysis mutation. *J. Neurosci.* **19,** 4762–4771 (1999).

Supplementary Information is linked to the online version of the paper at www.nature.com/nature.

Acknowledgements We thank J. W. Kyle, D. A. Hanck and A. L. Goldin for the $rNa_v1.2a$, $rNa_v1.4$ and β_1 clones, C. Deutsch for $K_v1.3$, M. M. Smith for GxTx-1E, K. M. Blumenthal and J. B. Herrington for ProTx-II, L. D. Possani for a sample of TsVII, the NINDS DNA sequencing facility for DNA sequencing, and the NINDS protein sequencing facility for mass spectrometry and peptide sequencing. We thank A. A. Alabi for helping with K_v and Na_v channel alignments and T.-H. Chang for assistance with Na_v channel mutants. We also thank A. A. Alabi, M. Holmgren, M. Mayer, M. Milescu, J. Mindell, A. Plested, S. Silberberg and members of the Swartz laboratory for discussions. This work was supported by the Intramural Research Program of the NINDS, NIH (K.J.S.) and by an NIH-FWO postdoctoral fellowship (F.B.).

Author Information Reprints and permissions information is available at www.nature.com/reprints. Correspondence and requests for materials should be addressed to K.J.S. (swartzk@ninds.nih.gov).

METHODS

Channel and chimaera constructs. Chimaeras and point mutations were generated using sequential polymerase chain reactions (PCR) with $K_v2.1\Delta7$ (refs 19, 51), $K_v1.3$ (ref. 52), Shaker (ref. 53), $rNa_v1.2a$ (neuronal type)[54] or $rNa_v1.4$ (muscle type)[55] as templates. Channel nomenclature consists of a numerical system in which the number following the subscript indicates the gene subfamily, followed by a number indicating the specific channel isoform. Splice variants of each family member are identified by lowercase letters following the numbers. For Nav channels the prefix 'r' indicates the organism (rat) from which the channel was cloned. The $K_v2.1\Delta7$ construct contains seven point mutations in the outer vestibule[19], rendering the channel sensitive to agitoxin-2, a pore-blocking toxin from scorpion venom[56]. The Shaker construct contains a deletion of residues 6–46 to remove inactivation[57]. The DNA sequence of all constructs and mutants was confirmed by automated DNA sequencing, and cRNA was synthesized using T7/SP6 polymerase (Message Machine kit, Ambion) after linearizing the DNA with appropriate restriction enzymes.

Spider and scorpion toxin purification. PaurTx3 (ref. 25) was purified from the venom of *Phrixotrichus auratus* (Spider Pharm) using a new two-step HPLC protocol (Supplementary Fig. 5a). Identity and purity were determined with mass spectrometry and automated peptide sequencing. Hanatoxin was purified from *Grammostola spatulata* venom (Spider Pharm) as described previously[58]. SGTx1 and VSTx1 were synthesized using solid-phase chemical methods, folded *in vitro* and purified as described previously[44,59]. AaHII from *Androctonus australis hector* venom (animals collected near Tozeur, Tunisia), and TsVII from *Tityus serrulatus* venom (gift from C. Diniz) were purified as described previously[60,61]. Synthetic ProTx-I was acquired from Peptides International. ProTx-II was provided by K. M. Blumenthal (SUNY) and J. B. Herrington (Merck Research Labs, Rahway). GxTx-1E was provided by M. M. Smith (Merck Research Labs, Rahway). The plant alkaloid veratridine (VTD; Sigma) is used as a negative control in Fig. 2 as the binding site of this lipid-soluble compound is thought to consist of the S6 transmembrane segments[62]. Toxins were kept at −20 °C. Before experiments, toxin aliquots were dissolved in appropriate solutions containing 0.1% BSA (or 1% BSA in the case of TsVII).

Two-electrode voltage-clamp recording from *Xenopus* oocytes. Channel constructs were expressed in *Xenopus* oocytes[21] and studied following 1–2 days incubation after cRNA injection (incubated at 17 °C in 96 mM NaCl, 2 mM KCl, 5 mM HEPES, 1 mM $MgCl_2$ and 1.8 mM $CaCl_2$, 50 μg ml^{-1} gentamycin, pH 7.6 with NaOH) using two-electrode voltage-clamp recording techniques (OC-725C, Warner Instruments) with a 150 μl recording chamber. Data were filtered at 1 kHz and digitized at 10 kHz using pClamp software (Axon). Microelectrode resistances were 0.1–1 MΩ when filled with 3 M KCl. For most K_v channel experiments, the external recording solution contained 50 mM KCl, 50 mM NaCl, 5 mM HEPES, 1 mM $MgCl_2$ and 0.3 mM $CaCl_2$, pH 7.6 with NaOH. KCl was replaced by RbCl for Shaker experiments. For Na_v channel experiments, the external recording solution contained 96 mM NaCl, 2 mM KCl, 5 mM HEPES, 1 mM $MgCl_2$ and 1.8 mM $CaCl_2$, pH 7.6 with NaOH. For Na_v channel experiments, oocytes were co-injected with the β_1 subunit in a 1:5 molar ratio. All experiments were performed at room temperature (~22 °C). Leak and background conductances, identified by blocking the channel with agitoxin-2, have been subtracted for all of the K_v channel currents shown[21]. Tetrodotoxin subtraction (TTX) or an online P/-4 prepulse protocol was used to subtract linear leak and membrane capacitive currents to isolate Na_v channel currents.

Analysis of channel activity and toxin–channel interactions. Voltage–activation relationships were obtained by measuring tail currents for K_v channels or steady-state currents and calculating conductance for Na_v channels, and a single Boltzmann function was fitted to the data according to $I/I_{max} = [1 + \exp(-zF(V - V_{1/2})/RT)]^{-1}$, where I/I_{max} is the normalized tail-current amplitude, z is the equivalent charge, $V_{1/2}$ is the half-activation voltage, F is Faraday's constant, R is the gas constant and T is temperature in kelvin.

Occupancy of closed or resting channels by toxins was examined using negative holding voltages where open probability was low, and the fraction of unbound channels (F_u) was estimated using depolarizations that are too weak to open toxin-bound channels, as described previously[17–21,24,44]. After addition of the toxin to the recording chamber, the equilibration between the toxin and the channel was monitored using weak depolarizations elicited at 5–10 s intervals. For all channels, we recorded voltage–activation relationships in the absence and presence of different concentrations of toxin. The ratio of currents (I/I_0) recorded in the presence (I) and absence (I_0) of toxin was calculated for various strength depolarizations, typically –70 mV to +10 mV. The value of I/I_0 measured in the plateau phase at voltages where toxin-bound channels do not open was taken as F_u (Supplementary Fig. 5b, c). The apparent equilibrium dissociation constant (K_d) for K_v channels was calculated according to $K_d = ((1/(1 - Fu^{1/4})) - 1)[\text{toxin}]$ assuming four independent toxin-binding sites per channel, with single occupancy being sufficient to inhibit opening in response to weak depolarizations. For all chimaeras and mutants, voltage protocols were adjusted appropriately so that the plateau phase in the I/I_0–voltage relationship was well defined. Example traces showing the inhibitory activity of tarantula toxins were taken for relatively weak depolarizations within the plateau phase for that particular channel construct. Off-line data analysis was performed using Clampfit (Axon), Origin 7.5 (Originlab) and Microsoft Solver (Microsoft Excel).

51. Frech, G. C., VanDongen, A. M., Schuster, G., Brown, A. M. & Joho, R. H. A novel potassium channel with delayed rectifier properties isolated from rat brain by expression cloning. *Nature* **340**, 642–645 (1989).
52. Stuhmer, W. *et al.* Molecular basis of functional diversity of voltage-gated potassium channels in mammalian brain. *EMBO J.* **8**, 3235–3244 (1989).
53. Tempel, B. L., Papazian, D. M., Schwarz, T. L., Jan, Y. N. & Jan, L. Y. Sequence of a probable potassium channel component encoded at Shaker locus of Drosophila. *Science* **237**, 770–775 (1987).
54. Auld, V. J. *et al.* A rat brain Na^+ channel alpha subunit with novel gating properties. *Neuron* **1**, 449–461 (1988).
55. Trimmer, J. S. *et al.* Primary structure and functional expression of a mammalian skeletal muscle sodium channel. *Neuron* **3**, 33–49 (1989).
56. Garcia, M. L., Garcia-Calvo, M., Hidalgo, P., Lee, A. & MacKinnon, R. Purification and characterization of three inhibitors of voltage-dependent K^+ channels from *Leiurus quinquestriatus* var. *hebraeus* venom. *Biochemistry* **33**, 6834–6839 (1994).
57. Hoshi, T., Zagotta, W. N. & Aldrich, R. W. Biophysical and molecular mechanisms of Shaker potassium channel inactivation. *Science* **250**, 533–538 (1990).
58. Swartz, K. J. & MacKinnon, R. An inhibitor of the Kv2.1 potassium channel isolated from the venom of a Chilean tarantula. *Neuron* **15**, 941–949 (1995).
59. Jung, H. J. *et al.* Solution structure and lipid membrane partitioning of VSTx1, an inhibitor of the KvAP potassium channel. *Biochemistry* **44**, 6015–6023 (2005).
60. Ceard, B., De Lima, M. E., Bougis, P. E. & Martin-Eauclaire, M. F. Purification of the main beta-toxin from *Tityus serrulatus* scorpion venom using high-performance liquid chromatography. *Toxicon* **30**, 105–110 (1992).
61. Martin, M. F., Rochat, H., Marchot, P. & Bougis, P. E. Use of high performance liquid chromatography to demonstrate quantitative variation in components of venom from the scorpion *Androctonus australis hector*. *Toxicon* **25**, 569–573 (1987).
62. Wang, G. K., Quan, C., Seaver, M. & Wang, S. Y. Modification of wild-type and batrachotoxin-resistant muscle mu1 Na^+ channels by veratridine. *Pflugers Arch.* **439**, 705–713 (2000).